Materials Letters 118 (2014) 99–102

Contents lists available at ScienceDirect

Materials Letters

journal homepage: www.elsevier.com/locate/matlet

Layer-by-Layer synthesis and tunable optical properties of hybrid magnetic–plasmonic nanocomposites using short bifunctional molecular linkers

Ward Brullot[a,*], Rik Strobbe[a], Maud Bynens[a], Maarten Bloemen[a], Pieter-Jan Demeyer[a], Willem Vanderlinden[a], Steven De Feyter[a], Ventsislav K. Valev[b], Thierry Verbiest[a]

[a] Molecular Imaging and Photonics, Department of Chemistry, KU Leuven, Celestijnenlaan 200D, Box 2425, 3001 Heverlee (Leuven), Belgium
[b] Cavendish Laboratory, Department of Physics, University of Cambridge, JJ Thomson Avenue, Cambridge CB30HE, United Kingdom

ARTICLE INFO

Article history:
Received 19 October 2013
Accepted 11 December 2013
Available online 19 December 2013

Keywords:
Nanocomposite
Layer-by-Layer
Magnetic–plasmonic
Nanoparticle
Tunable optical property

ABSTRACT

Spurred by research in magnetoplasmonics, plasmon-enhanced magneto-optical effects and active plasmonics, the demand for hybrid magnetic–plasmonic nanoparticle-based materials of optical quality is high. Currently used synthesis methods involve possibly interfering polymer media or polyelectrolyte interlayers, grooved supports or non-transparent substrates. To obtain homogeneous, partially transparent and polymer/polyelectrolyte-free magnetic–plasmonic nanocomposites with angle-independent optical properties, we produced hybrid gold–magnetite and silver–magnetite nanocomposites by a novel Layer-by-Layer synthesis using short bifunctional molecular linkers on glass substrates. Resulting nanocomposites had high nanoparticle filling fractions and showed tunability of the plasmon wavelength over a very broad spectral range by changing composite thickness through the number of added nanoparticle layers. The angle-independence of optical properties and the abilities to switch the plasmonic material and to tune the plasmon resonances of the magnetic–plasmonic composites make these materials a unique platform for magnetoplasmonic research.

1. Introduction

Research into nanoparticle-based magnetoplasmonics, active plasmonics and plasmon-enhanced magneto-optics has strongly intensified [1–5]. Such research holds promise for both unraveling fundamental questions about magnetic–plasmonic interactions as well as applications in sensing, optical switching and optical components fabrications. The ability to reliably synthesize high optical quality magnetic–plasmonic nanocomposites with high nanoparticle filling fractions and without introducing unnecessary background signal facilitates experiments and is a prerequisite to interpret results correctly. Furthermore, for many experiments or applications, such as optical Faraday isolators, (partial) transparency is a must [3,6]. Previously, nanocomposites were synthesized on non-transparent or grooved substrates [5] using polymers as a dispersion medium for spin-coated or drop-casted samples or polyelectrolyte interlayers in Layer-by-Layer synthesis [7–9]. Polymers and polyelectrolytes have the disadvantages that nanoparticle filling fractions are inherently limited and that they possibly introduce undesired background signal, chemical incompatibility and interfere with signal acquisition. Furthermore, such molecules introduce an undefined and often large distance between adjacent nanoparticles, impeding correct interpretation of results. Here we present a versatile Layer-by-Layer synthesis method on glass substrates using short bifunctional, i.e. with two functional groups, molecular linkers that results in homogeneous samples with very high nanoparticle filling fractions and controlled distances between adjacent particles. Tunable plasmon properties, of both silver– and gold–magnetite nanocomposites, over a broad spectral range combined with angle-independent optical properties and a variable composite thickness make these high quality composites an ideal platform for magneto-plasmonic research.

2. Materials and methods

Materials: All obtained chemicals were used without further purification. Anhydrous iron(III)trichloride (98%), n-octylamine (99+%) and ethanediol (for analysis) were purchased from Acros Organics. (3-Aminopropyl)trimethoxysilane (APTMS; 97%) was obtained from ABCR. Gold(III)chloride trihydrate (99.9+%), sulfuric acid (95–97%) and Nochromix cleaning agent were purchased from Sigma-Aldrich. Acetic acid (100%) was bought from VWR, silver nitrate from UCB, tri-sodium citrate (99.5+%) from Chem-Lab and

---

* Corresponding author. Tel.: +32 1632 7154.
E-mail address: ward.brullot@fys.kuleuven.be (W. Brullot).

0167-577X/$ - see front matter © 2013 Elsevier B.V. All rights reserved.
http://dx.doi.org/10.1016/j.matlet.2013.12.057

sodium borohydride (98+%) from Janssen Chemica.*Methods of iron oxide nanoparticle synthesis*: Iron oxide nanoparticles were synthesized using an in-house modified force hydrolysis method [10]. XRD experiments showed that the dominant iron oxide phase was magnetite (Supplementary information).

Methods of functionalization of iron oxide nanoparticles: 300 mg of n-octylamine coated nanoparticles was dispersed in 300 ml methanol using an ultrasonic bath. Then 3 ml APTMS was added, together with three drops of acetic acid and the mixture was further sonicated for 2 h. After washing with acetone through magnetically assisted precipitation and drying in vacuum, a powder of amine-functionalized iron oxide nanoparticles was obtained. These functionalized nanoparticles could then be redispersed in MeOH in a desired concentration using ultrasonication. Functionalized particles had a size of 7.98 ± 2.4 nm and showed superparamagnetic behavior with a saturation magnetization of 18.88 emu/g (Supplementary information).

Methods of synthesis of metal nanoparticles: For the gold colloid synthesis, a method based on an aqueous citrate reduction was employed [11]. After synthesis, a deep red colored dispersion was obtained. This dispersion was diluted 5 × with MilliQ water before use to obtain a final Au concentration of 0.2 mM. Au nanoparticles had a size of 9.25 ± 1.31 nm and exhibited a clear plasmon resonance centered on 530 nm (Supplementary information). Silver nanoparticles were produced using a method based on an aqueous sodium borohydride reduction in the presence of citrate capping molecules [12]. The pale yellow colored dispersion was used without further dilution. Ag nanoparticles showed a plasmon resonance at 400 nm and had a size of 9.59 ± 0.27 nm as measured by TEM (Supplementary information). Final Ag concentration was 0.15 mM.

Methods of synthesis of nanocomposites (Fig. 1A–D): Synthesis started by cleaning glass microscope slides (16 × 16 mm^2) with NoChromix cleaning solution (7 g/100 ml NoChromix in MilliQ water, add 100 ml sulfuric acid 97%) for 1 h. These cleaned substrates were then functionalized with APTMS (1 vol% in MeOH, 1 h) and rinsed with MeOH and water [11]. A first metal nanoparticle layer was added by putting the functionalized substrate in 10 ml of a metal NP dispersion while shaking (350 rpm) for 1.5 h and rinsing with water and MeOH afterwards. By putting the sample in 10 ml of a 0.3 mg/ml dispersion of functionalized iron oxide nanoparticles in MeOH for 1 h, a layer of these nanoparticles could be added on top of the gold nanoparticle layer. After rinsing the sample with methanol and water, adding extra nanoparticle layers was possible by repeating the previous steps. The nature of the Layer-by-Layer synthesis allows for homogeneous coating of large-area substrates.

Methods of characterization: Nanoparticles and composites were characterized using transmission electron microscopy (80 kV Zeiss EM-900, 300 mesh Formvar on copper grids as substrate), scanning electron microscopy (XL30 ESEM FEG microscope), room temperature X-ray diffraction experiments (horizontal Geigerflex diffractometer in Bragg–Brentano geometry reflection mode, mounted on a Rigaku RU-200B rotating Cu-anode with an output power of 4 kW), vibrating sample magnetometry (300 K, Oxford instruments VSM Maglab), scanning force microscopy (multimode 8 from Bruker using an AC240TS tip) and UV–visible absorbance measurements (Perkin-Elmer 900).

3. Results and discussion

Au–magnetite nanocomposites with different numbers of nanoparticle double layers (NDLs), which were one gold and one iron oxide nanolayer combined (Fig. 1D), were synthesized. A five NDLs Au–magnetite composite on a glass support is blue colored when viewed perpendicular and shows gold reflectivity if tilted. The sample is homogeneous, showing no large aggregates or defects (Fig. 1E, inset). Scanning electron microscopy (SEM) images confirm homogeneity over at least 100 µm and show a relatively smooth surface (Fig. 1E). When zoomed in on the same sample next to a scratch, a clear height difference between substrate and sample can be observed (Fig. 1F).

Due to the strong bonding between the silane group and the iron oxide nanoparticles on the one and the amine group of the linker molecule and the gold nanoparticles on the other hand, the samples are robust and do not release material in the storage solvent [10,11]. Stored in methanol, the composites were stable for at

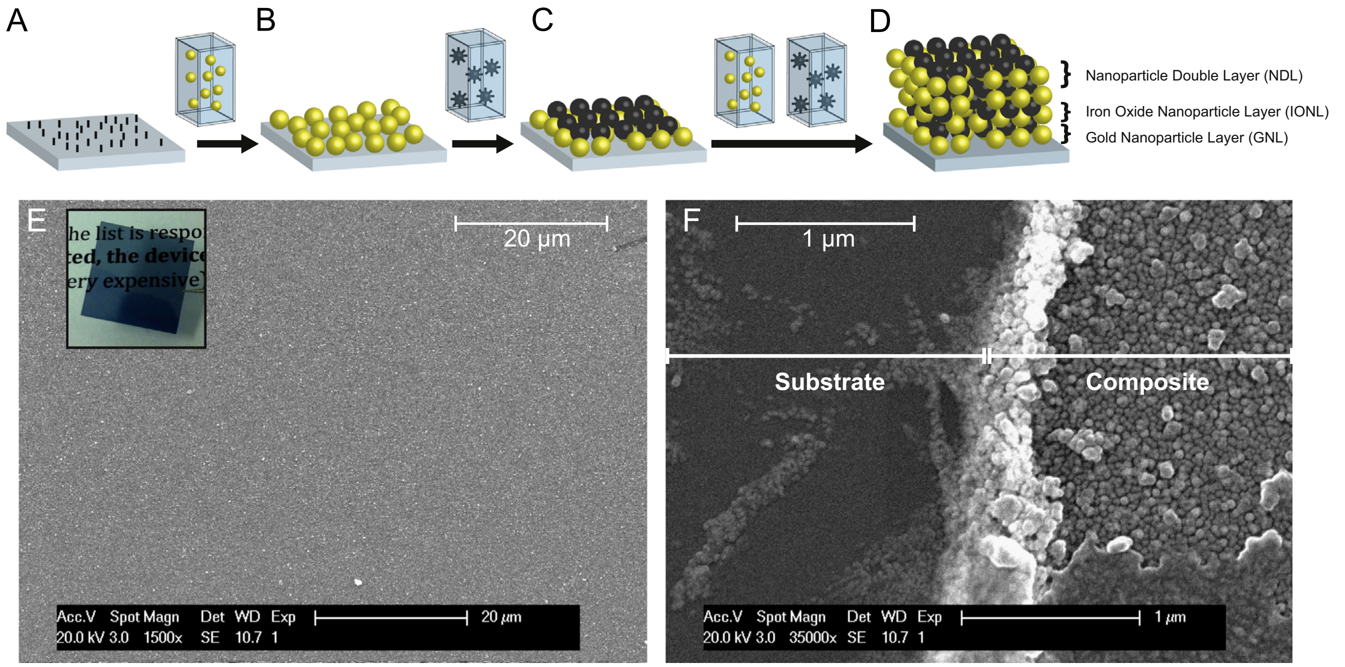

Fig. 1. Layer-by-Layer synthesis procedure used in this work (A)–(D), a photograph of a five NDLs Au–Mag sample above a text (inset E) and large area (E) and zoomed-in (F) scanning electron microscopy images of a Au–Mag five NDLs sample.

least 1 year as evidenced by UV–visible absorbance spectroscopy. Ultrasonic treatment of five NDLs Au–magnetite composite does not result in any change in the UV–visible absorbance spectrum, indicating the stability and robustness of the samples. Reproducibility of the method is high (Supplementary information).

UV–visible absorbance spectra of a one NDL Au–magnetite nanocomposite show a plasmon resonance peak at approximately 520 nm, corresponding to that of dispersed gold nanoparticles (Fig. 2). By adding NDLs, a second redshifted plasmon peak due to plasmonic near-field coupling arises. When gold nanoparticles interact optically, the plasmon modes couple, resulting in redshifts of the plasmon wavelength [13]. The observed significant redshift of the plasmon wavelength in the synthesized samples from 530 nm to 650 nm indicates that gold nanoparticles are interacting strongly and thus are close to each other. The presence of magnetite nanoparticles is evidenced by the absorbance peak due to intervalence charge transfer (IVCT) centered around 385 nm [14]. A linear relationship between the absorbance maximum and the number of layers was found (Fig. 3), evidencing the Layer-by-Layer synthesis of the composites. The same linear relationship was found for the absorbance at the iron oxide NP IVCT and the Au LSPR and coupled plasmon modes as a function of NDLs (Supplementary information). Changes in the UV–visible absorbance spectra as a function of added NDLs can be visually observed as a change in color of the Au–magnetite composites from reddish pink over blue to dark blue with increasing number of NDLs. Use of glass substrates allows for partial transparency of the composites in the UV–visible, enabling magnetoplasmonic and magneto-optical measurements and applications.

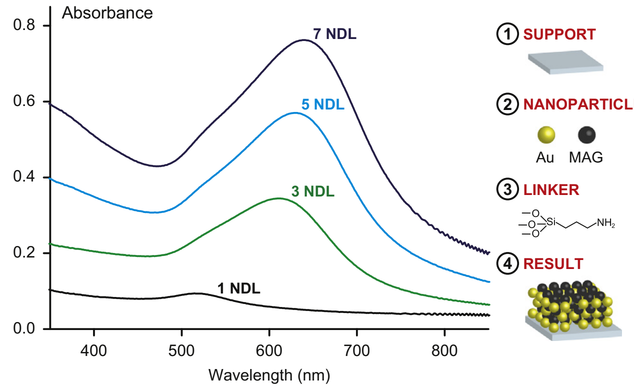

Fig. 2. UV–visible absorbance spectra of Au–Mag composites show a redshift of the localized surface plasmon band as a function of added NDL. The presence of magnetite nanoparticles is indicated by the resonance at 385 nm.

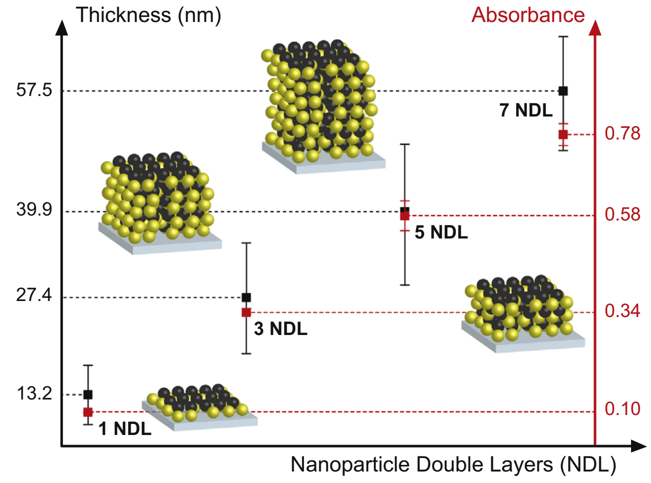

Fig. 3. Both the thickness, as measured by scanning force microscopy, and the absorbance at maximum intensity increase linearly with increasing number of nanoparticle double layers. These results demonstrate the Layer-by-Layer construction of the Au–Mag composites.

The absorbance properties of the composites, including the plasmon properties, are largely independent of the sample angle relative to the incoming light beam (Supplementary information), which is in stark contrast to the strong angle dependence of propagating plasmon resonance excitation of continuous bulk gold layers [3,15]. Lyon et al. observed that the strict angle requirements for exciting surface plasmon modes in continuous gold layers can be partially lifted by covering the surface with gold colloids [16]. In the synthesized composites, only spherical gold nanoparticles are responsible for the plasmon behavior, which fully alleviates the incident angle requirements. Angle independent optical properties can be a great advantage for (magneto-)optical experiments and applications.

The average thickness of the Au–magnetite nanocomposites, as measured by scanning force microscopy (Supplementary information), increases linearly with the number of added NDLs. This confirms the Layer-by-Layer like construction (Fig. 3). A thickness of 13.2 ± 7.3 nm was measured for a one NDL sample. When fitted with a linear equation ($R^2 = 0.99$), the average increase of thickness for one NDL after the first NDL is 7.3 ± 0. 4 nm. These data are consistent with structures in which, resembling a closed-packed material, the nanoparticles of the next nanoparticle layers occupy the cavities in the previous and a high quality stacking of layers is obtained (graphics Fig. 3). Structures with such a packed arrangement of nanoparticles allow a high nanoparticle filling fractions or occupied volume fractions up to, in the case of fully close-packed arrangements, a theoretical maximum of 74% [17]. The number of layers that can be added is in principle unlimited, although some quality loss is likely with very high numbers of layers. Up until 10 NDLs no loss of optical quality was observed (Supplementary information). Such structures with high nanoparticle filling, and the absence of polymer, polyelectrolyte or other possibly interfering interlayers and of high optical quality are well suited for studying plasmon-enhanced effects or investigating fundamentals of active plasmonics.

Using silver instead of Au nanoparticles in the Layer-by-Layer synthesis also results in stable and homogeneous nanocomposites. The UV–visible absorbance spectra of such composites show only two absorbance bands (Fig. 4). One broad band is centered on 400 nm due to the overlap of the IVCT and plasmon resonances of magnetite and single Ag nanoparticles. When more than one NDL is added, a strongly redshifted plasmon band at around 550–575 nm occurs due to near-field optical coupling of Ag

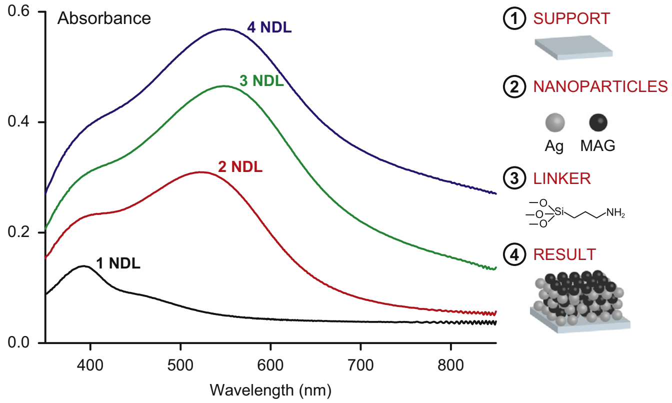

Fig. 4. A strong redshift of the plasmon wavelength is observed in UV–visible absorbance spectra of Ag–Mag composites. The resonance of magnetite nanoparticles (385 nm) overlaps with the LSPR of Ag NP.

nanoparticles. The same as for the Au-based composites, a linear relationship between the absorbance maximum and the number of layers was found (Supplementary information), evidencing the Layer-by-Layer synthesis of the composites.

The abilities to switch the plasmonic material and to tune the plasmon resonances of the magnetic–plasmonic composites over a very broad UV–visible spectral range as a function of added NDLs provide a unique platform for magnetoplasmonic research.

4. Conclusion

Magnetic–plasmonic nanocomposites of optical quality and variable thickness based on Au or Ag and magnetite nanoparticles were reproducibly synthesized on glass substrates by a polymer/polyelectrolyte-free Layer-by-Layer method using short bifunctional molecular linkers. High nanoparticle filling fractions in well-stacked multilayers were obtained. Plasmon resonance wavelengths could be tuned over a very broad spectral range by changing the plasmonic material or the number of added nanoparticle layers. Optical properties proved to be angle-independent. Such high quality composites without possibly interfering interlayers provide excellent materials for research into plasmon influenced (magneto-)optical effects, active plasmonics through magnetism or possibly magnetoresistance effects.

Acknowledgments

The authors thank Prof. J. Billen of the KU Leuven for help with the transmission electron microscopy images and the Department of Metallurgy and Materials Engineering of the KU Leuven for access to Scanning Electron Microscopy. The authors are grateful to M. Vanbel and S. Vandendriessche of the Division Molecular Visualization and Photonics of the KU Leuven for inspiring discussions on the topic and critical reading of the manuscript. W. Brullot and M. Bloemen are grateful for a Ph.D. grant by the Agency for Innovation by Science and Technology (IWT) Flanders. PJ. Demeyer thanks the Department of Chemistry of the KU Leuven for a FLOF Grant. V.K. Valev acknowledges financial support from the EPSRC Grant EP/G060649/1. T. Verbiest and S. De Feyter acknowledge support from the KU Leuven (GOA Research Grant). T. Verbiest acknowledges the FWO-Vlaanderen for financial support through Research project G.0C02.13N.

Appendix A. Supporting information

Supplementary data associated with this article can be found in the online version at http://dx.doi.org/10.1016/j.matlet.2013.12.057.

References

[1] Dani RK, Wang H, Bossmann SH, Wysin G, Chikan V. Faraday rotation enhancement of gold coated Fe_2O_3 nanoparticles: comparison of experiment and theory. J Chem Phys 2011;135:224502.

[2] Jain PK, Xiao Y, Walsworth R, Cohen AE. Surface plasmon resonance enhanced magneto-optics (SuPREMO): Faraday rotation enhancement in gold-coated iron oxide nanocrystals. Nano Lett 2009;9:1644–50.

[3] Armelles G, Cebollada A, García-Martín A, González MU. Magnetoplasmonics: combining magnetic and plasmonic functionalities. Adv Opt Mater 2013;1:10–35.

[4] Armelles G, Cebollada A. Magneto-optical properties of core – shell magneto-plasmonic $Au - Co_xFe_{3-x}O_4$ nanowires. Langmuir 2012:4–7.

[5] Caminale M, Anghinolfi L, Magnano E, Bondino F, Canepa M, Mattera L, et al. Tuning the magneto-optical response of iron oxide nanocrystals in Au- and Ag-based plasmonic media. ACS Appl Mater Interfaces 2013;5:1955–60.

[6] Chin JY, Steinle T, Wehlus T, Dregely D, Weiss T, Belotelov VI, et al. Nonreciprocal plasmonics enables giant enhancement of thin-film Faraday rotation. Nat Commun 2013;4:1599.

[7] Pichon BP, Louet P, Felix O, Drillon M, Begin-colin S, Decher G. Magnetotunable hybrid films of stratified iron oxide nanoparticles assembled by the layer-by-layer technique. Chem Mater 2011;23:3668–75.

[8] Wouters J, Lebedev OI, Van Tendeloo G, Yamada H, Sato N, Vanacken J, et al. Preparing polymer films doped with magnetic nanoparticles by spin-coating and melt-processing can induce an in-plane magnetic anisotropy. J Appl Phys 2011;109:076105.

[9] Vandendriessche S, Valev VK, Verbiest T. Characterization of magnetization-induced second harmonic generation in iron oxide polymer nanocomposites. Appl Opt 2012;51:209–13.

[10] Brullot W, Reddy NK, Wouters J, Valev VK, Goderis B, Vermant J, et al. Versatile ferrofluids based on polyethylene glycol coated iron oxide nanoparticles. J Magn Magn Mater 2012;324:1919–25.

[11] Keating CD, Musick MD, Keefe MH, Natan MJ. Kinetics and thermodynamics of Au colloid monolayer self-assembly: undergraduate experiments in surface and nanomaterials chemistry. J Chem Educ 1999;76:949.

[12] Tejamaya M, Römer I, Merrifield RC, Lead JR. Stability of citrate, PVP, and PEG coated silver nanoparticles in ecotoxicology media. Environ Sci Technol 2012;46:7011–7.

[13] Jain PK, El-Sayed MA. Plasmonic coupling in noble metal nanostructures. Chem Phys Lett 2010;487:153–64.

[14] Fontijn WFJ, van der Zaag PJ, Devillers MAC, Brabers VAM, Metselaar R. Optical and magneto-optical polar Kerr spectra of Fe_3O_4 and Mg^{2+}- or Al^{3+}-substituted Fe_3O_4. Phys Rev B 1997;56:5432–42.

[15] Gwon HR, Lee SH. Spectral and angular responses of surface plasmon resonance based on the Kretschmann prism configuration. Mater Trans 2010;51:1150–5.

[16] Lyon LA, Pen DJ, Natan MJ. Surface plasmon resonance of Au colloid-modified Au films: particle size dependence. J Phys Chem B 1999:5826–31.

[17] Hales TC, Ferguson SP. The Hales–Ferguson proof. In: Lagarias JC, editor. The Kepler conjecture. Springer; 2011, http://www.springer.com/mathematics/geometry/book/978-1-4614-1128-4.